Supplementary Information

Isotope effect on the spin dynamics of single-molecule magnets probed by muon spin spectroscopy

L. Tesi,[a] Z. Salman,[b*] I. Cimatti,[a] F. Pointillart,[c] K. Bernot,[c] M. Mannini[a] and R. Sessoli[a]*

[a] *Department of Chemistry "U. Schiff" - Università degli Studi di Firenze and INSTM UdR Firenze, Via della Lastruccia 3, 50019, Sesto Fiorentino, Italy.*

[b] *Laboratory for Muon Spin Spectroscopy, Paul Scherrer Institute, CH-5232 Villigen PSI, Switzerland.*

[c] *Université de Rennes, INSA Rennes, CNRS, ISCR (Institut des Sciences Chimiques de Rennes) - UMR 6226, 35000 Rennes, France.*

Corresponding authors email: roberta.sessoli@unifi.it and zaher.salman@psi.ch

Methods

The synthesis and purification of $[^{161/164}Dy(tta)_3(L)]\cdot C_6H_{14}$ (**^{161}Dytta** and **^{164}Dytta**) were performed following the procedure reported in literature,[1,2] starting from enriched Dy_2O_3 purchased from Eurisotop with the isotope contents reported in Table S1. The products appear as red microcrystalline powders. Powder X-Ray diffraction (PXRD) analyses were performed (Figure S1) on the same non-grounded samples used for the μSR measurements. For this, a *Bruker New D8 Advance DAVINCI* diffractometer equipped with a linear detector was used. Recording conditions with Cu K_α (λ=1.542 Å) in ϑ-2ϑ mode with 40 kV, 40 mA, step size 0.003°, scan speed 0.005°/s and a slit of 0.6 mm. The simulated pattern has been obtained with Mercury 3.0 from CCDC. While the isostructurality is guaranteed from single-crystal XRD measurements (see ref. 2), the PXRD spectra in Figure S1 indicate the same structural phase and the absence of impurities. Minor differences in the intensities of the peaks can be attributed to different orientations of the crystallites in the non-grounded samples.

Table S1 – Isotope contents for **^{161}Dytta** and **^{164}Dytta** determined by ICP-MS in Eurisotop Laboratories. The nuclear spin value, *I*, of the corresponding isotope is also reported.

Isotope	**156 (*I*=0)**	**158 (*I*=0)**	**160 (*I*=0)**	**161 (*I*=5/2)**	**162 (*I*=0)**	**163 (*I*=5/2)**	**164 (*I*=0)**
^{161}Dytta Content %	<0.1	<0.1	0.49	92.20	5.48	1.17	0.66
^{164}Dytta Content %	<0.01	<0.01	0.03	0.34	0.58	2.25	96.8

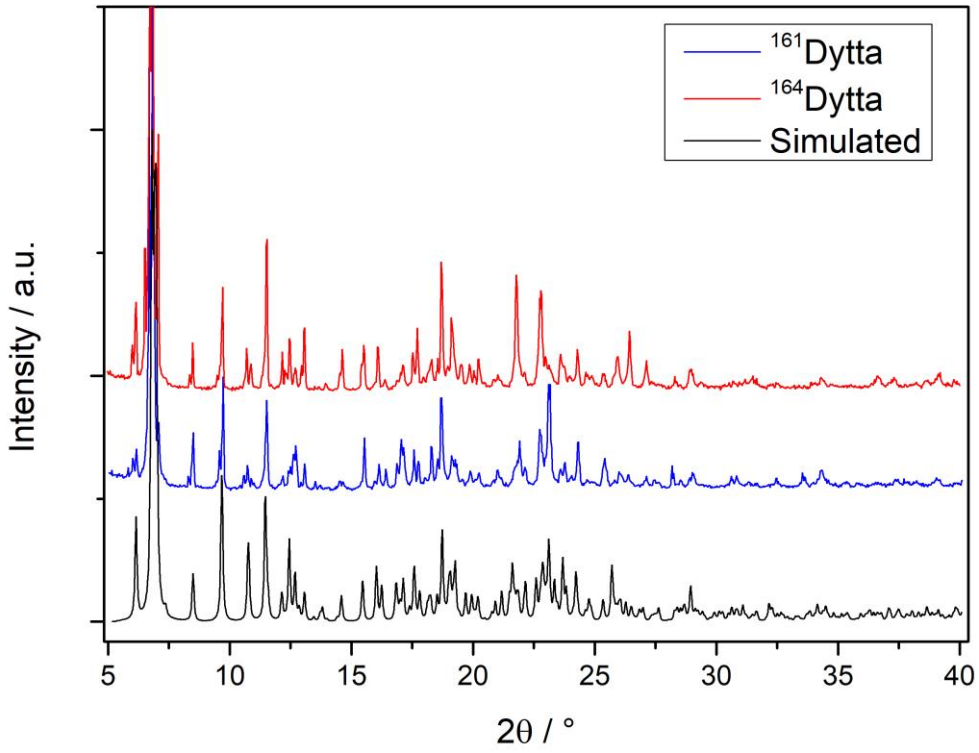

Figure S1: X-Ray powder diffraction pattern of **^{161}Dytta** (blue) and **^{164}Dytta** (red) measured at room temperature and comparison with simulated pattern from the crystal structure (150 K) of the genuine $[Dy(tta)_3(L)]\cdot C_6H_{14}$ sample made of natural Dy^{III}.[1]

For μSR experiments ca. 100 mg of **^{161}Dytta** and **^{164}Dytta** microcrystalline powders were wrapped and sealed in an aluminized Mylar foil with dimensions ca. 0.5x0.5x0.3 cm. The latter was then mounted on the sample holder and placed in a He flow cryostat at the GPS spectrometer of the Paul Scherrer Institute (PSI). The raw μSR asymmetry, $A_0P_Z(t)$, was measured in zero field (ZF mode) as a function of temperature, with the initial muon spin polarization rotated ca. 45° relative to the beam axis. Here A_0 is the initial asymmetry and $P_z(t)$ is the muon spin polarization. The raw asymmetry data were fit using $P_z(t)$ given by Equation 1. For each compound we assume that A_0 is a common and temperature independent parameter while allowing only λ and Δ to change with temperature. The best-fit A_0 parameters for **^{161}Dytta** and **^{164}Dytta** are A_0=0.141(1) and 0.145(1), respectively. In Figure S2 and S3 we plot the normalized $P_Z(t)$ curves for three different temperatures to highlight the time dependence in the three different regimes mentioned in the main text. In Figure S4 and S5 $P_Z(t)$ curves at all measured temperatures are shown.

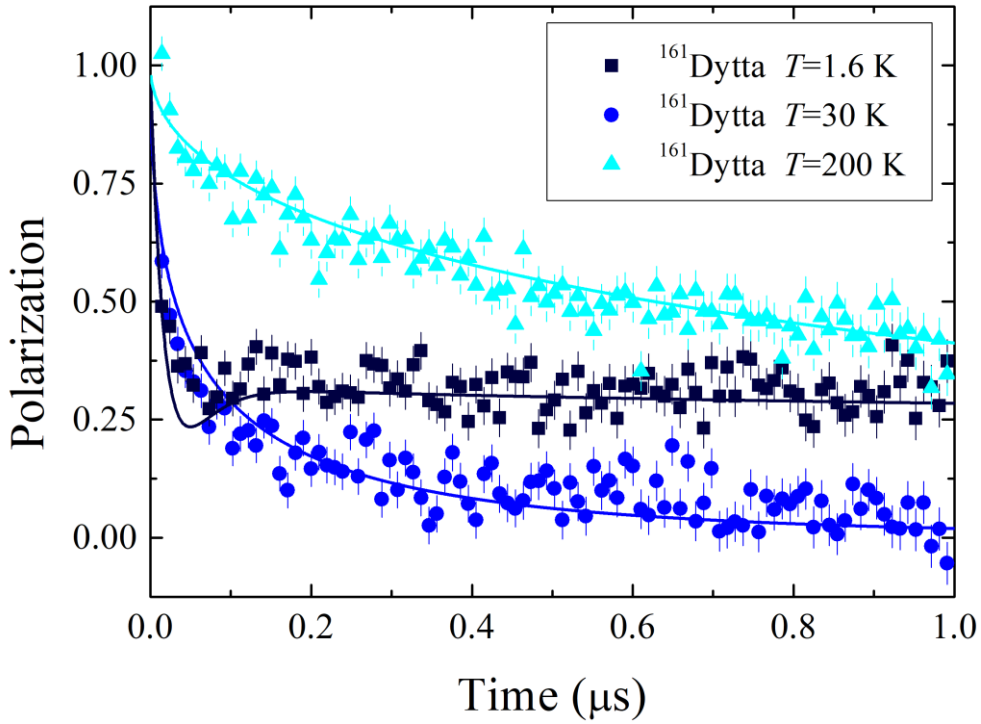

Figure S2: Examples of muon spin polarization, $P_Z(t)$, curves at three different temperatures for **^{161}Dytta** (scatter) in zero field. The polarization has been normalized to highlight the different ratios of the decays in the three regimes. The solid lines represent the best fits using a phenomenological Kubo-Toyabe model multiplied by a square root exponential relaxation function (Equation 1).

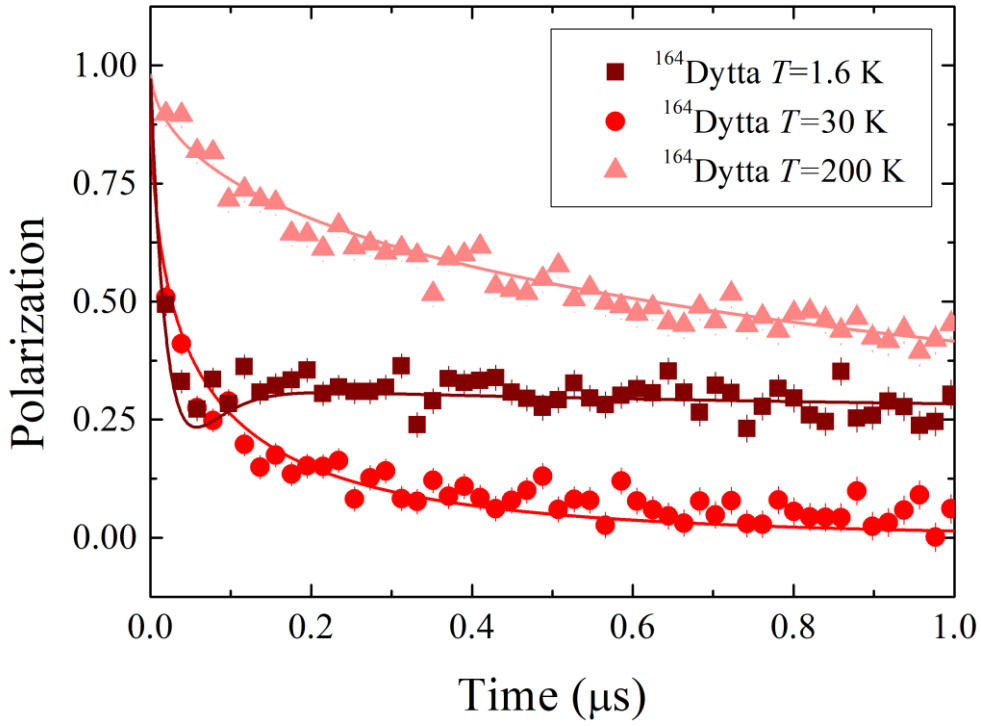

Figure S3: Examples of muon spin polarization, $P_Z(t)$, curves at three different temperatures for **^{164}Dytta** (scatter) in zero field. The polarization has been normalized to highlight the different ratios of the decays in the three regimes. The solid lines represent the best fits using a phenomenological Kubo-Toyabe model multiplied by a square root exponential relaxation function (Equation 1).

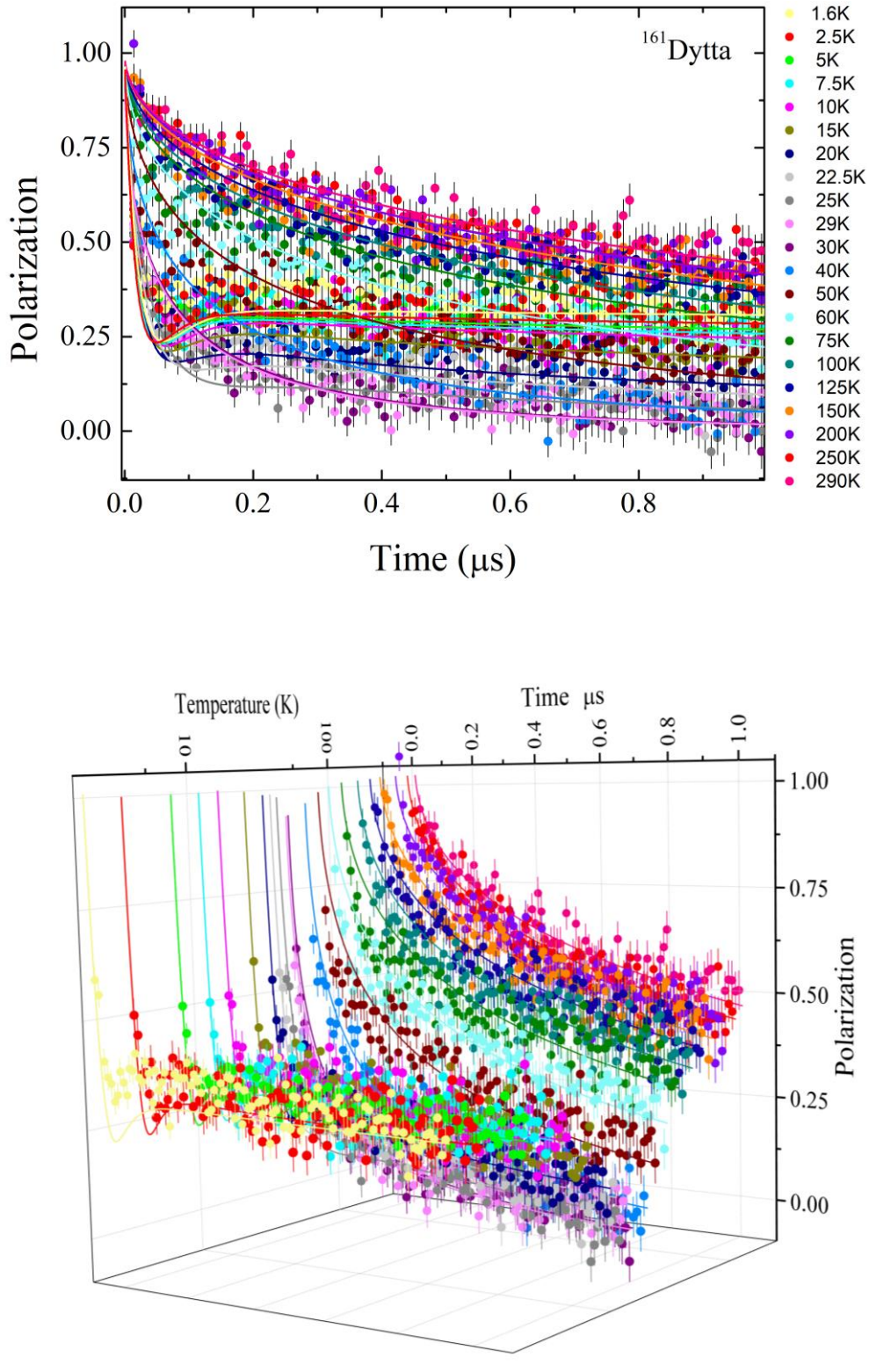

Figure S4: Muon spin polarization, $P_Z(t)$, curves at all measured temperatures for **^{161}Dytta** (scatter) in zero field, in two-dimensional (top) and three-dimensional (bottom) views. The polarization has been normalized to highlight the different ratios of the decays in the three regimes. The solid lines represent the best fits using a phenomenological Kubo-Toyabe model multiplied by a square root exponential relaxation function. In the 3D view the temperature is in log scale.

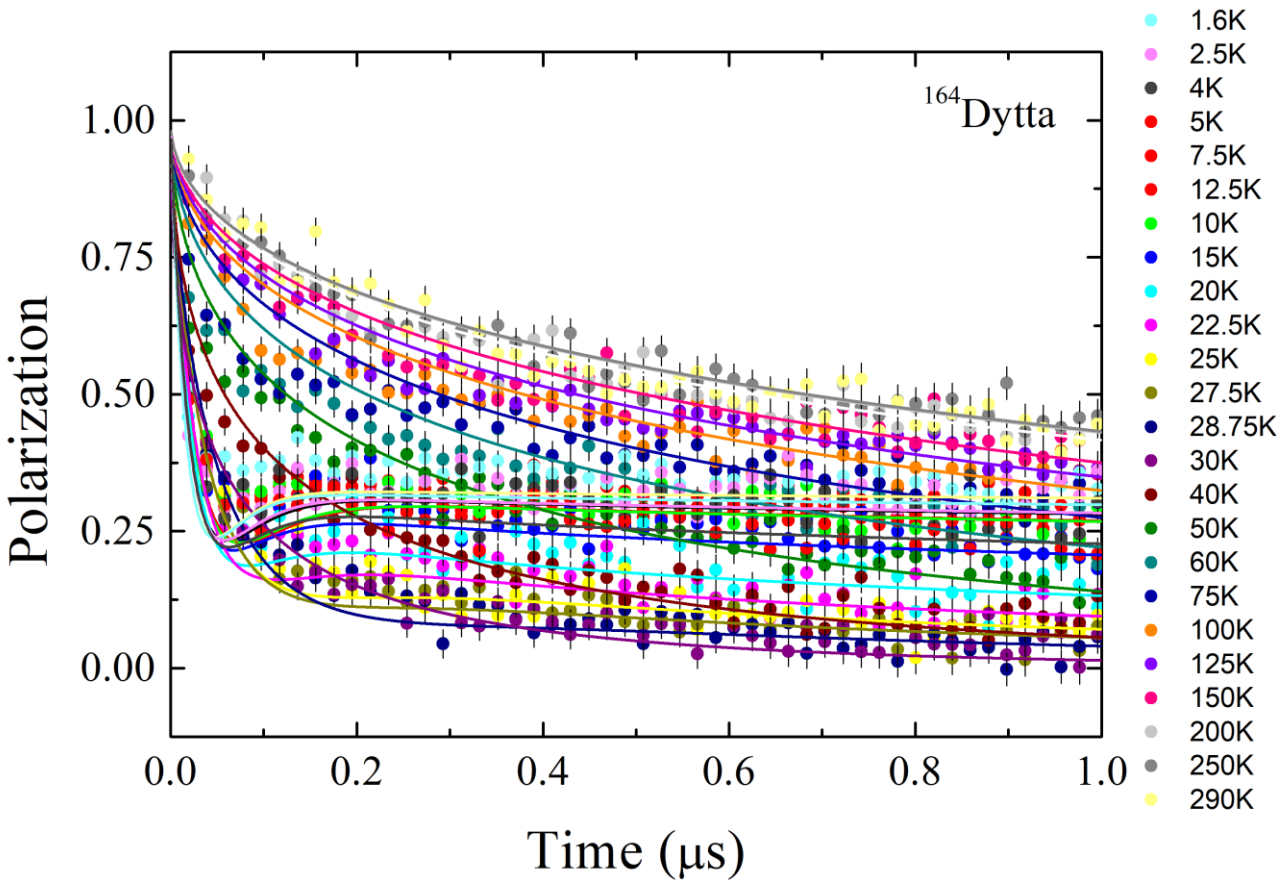

Figure S5: Muon spin polarization, $P_Z(t)$, curves at all measured temperatures for **^{164}Dytta** (scatter) in zero field. The polarization has been normalized to highlight the different ratios of the decays in the three regimes. The solid lines represent the best fits using a phenomenological Kubo-Toyabe model multiplied by a square root exponential relaxation function.

Careful calibration measurements in 3 mT transverse field (TF) and relatively high temperature, to evaluate the diamagnetic fraction of the muons in these compounds, give similar A_0 values to those obtained from the ZF measurements. These are also compared to measurements on a small silver sample (4x4 mm^2) under the same conditions, for which A_0=0.195(1) (Figure S6). Therefore, the observed signal amplitude detected in **Dytta** samples corresponds to ∽75% diamagnetic fraction. The missing ∽25% are most probably due to muonium (Mu) formation in the Mylar wrapping, or possibly in the **Dytta** sample itself. Nevertheless, Mu formation, whether in the sample or the Mylar, does not contribute to the measured signal since these muons depolarize almost immediately in ZF, leaving only the diamagnetic signal that we eventually observe. Our analysis of the ZF data shows that the geometric efficiency ratio of the positron detectors, α, and the initial asymmetry are equal to those extracted from the calibration measurement (with zero background signal). This confirms that the missing muons fraction (25%) is depolarized completely at early times and does not contribute to our measurements. Moreover, the Mu formation could not be responsible of the difference in the spin dynamics between the two samples, since it will be the same in the two chemically equivalent but isotopically enriched **Dytta** samples and it should not depend on temperature.

The used fitting function (Equation 1) reproduces the data quite well for times $t>0.2$ μs, though it sometimes misses the data at earlier times, in particular at low temperatures. Attempts to fit the data using other models, *e.g.* the sum of two exponentials, give parameters with unphysical values. Therefore, the use of the modified Kubo-Toyabe model provides a most suitable and satisfactory fit with a small number of free parameters. We also note that the values of Δ extracted from the data are quite large and at the limit of what we can currently measure with μSR. In addition, **Dytta** molecules contain many oxygen and fluorine ions,

presenting a much more negatively charged and attractive environment for the muon to stop in. These muons are close to the Dy^{III} ion (see Figure 1) and therefore they sense its dipolar field. The multiple stopping sites in these molecular systems result in a very broad and sometimes unusual local field distribution. This latter cannot be accounted for by a simple Lorenzian function which would produce an even shallower dip in the spectra, as shown in Figures S2 and S3. However, the dip and values of Δ do not affect the relaxation rate λ, *i.e.* the slope of the 1/3 tail, and the corresponding correlation time τ at low temperatures. As such, they will not affect our primary conclusion concerning the difference in τ at low temperatures, which we attribute to the effect of Dy^{III} nuclear moments on the dynamics of its electronic spin.

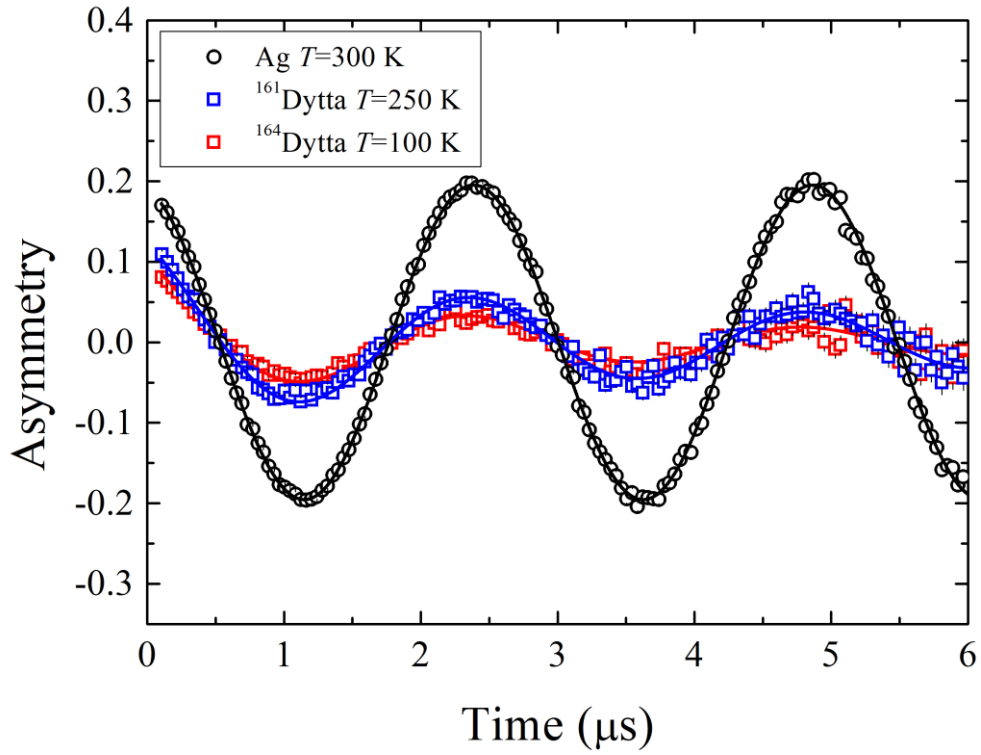

Figure S6: Comparison of the calibration measurements of muon spin polarization, $P_Z(t)$, asymmetries for **^{161}Dytta**, **^{164}Dytta** and a reference sample of Ag. The measurements are performed in 3 mT of transverse field and relatively high temperature.

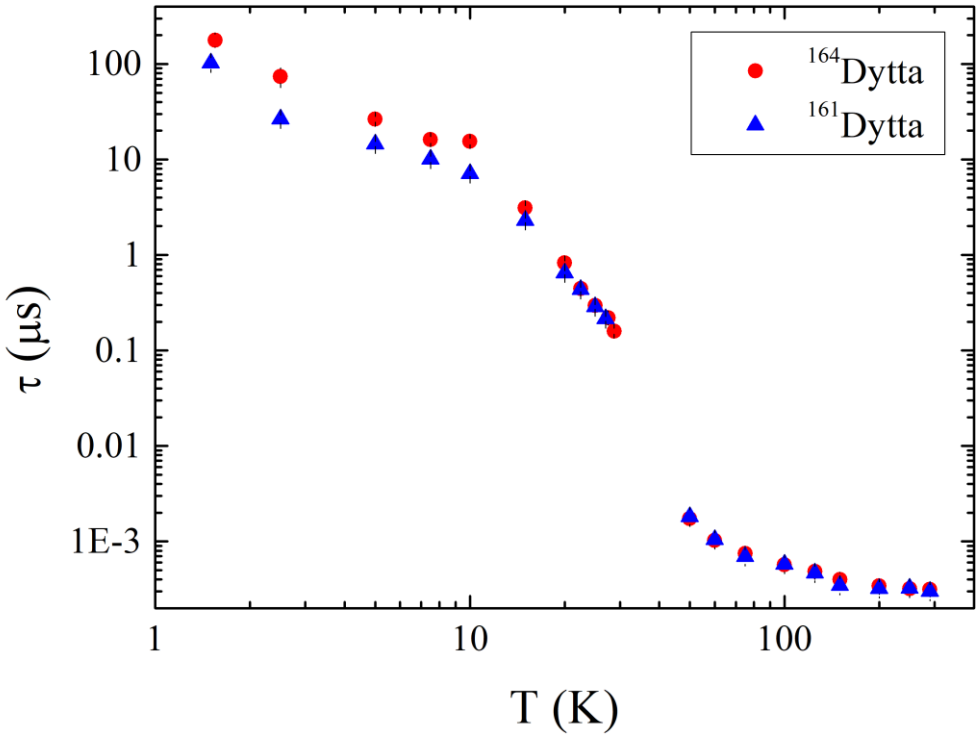

Figure S7: Temperature dependence of the correlation time extracted from μSR for **^{161}Dytta** and **^{164}Dytta** in the whole investigated temperature range. Data are reported in log-log scale.

References

1. T. T. da Cunha, J. Jung, M.-E. Boulon, G. Campo, F. Pointillart, C. L. M. Pereira, B. Le Guennic, O. Cador, K. Bernot, F. Pineider, S. Golhen and L. Ouahab, *J. Am. Chem. Soc.*, 2013, **135**, 16332-16335.

2. F. Pointillart, K. Bernot, S. Golhen, B. Le Guennic, T. Guizouarn, L. Ouahab and O. Cador, *Angew. Chem. Int. Ed.*, 2015, **54**, 1504-1507.